

An Evaluation of CubeSat Orbital Decay

Daniel L. Oltrogge
 Analytical Graphics, Inc.
 7150 Campus Dr., Suite 260, Colorado Springs, CO 80919 ; 610-981-8616
 Oltrogge@AGLcom

Kyle Leveque
 SRI, Inc.
 333 Ravenswood Ave, Menlo Park, CA 94025-3493; 650-859-4621
 kyle.leveque@sri.com

ABSTRACT

Accurate orbit lifetime assessment is necessary to support satellite mission design, concepts-of-operation, and post-mission debris mitigation strategies. Because of their standardized form factors, the 47 CubeSats placed in orbit since 2003 provide a unique opportunity to study the accuracy of such orbit lifetime techniques in a controlled manner. In this study we examine CubeSat assessments for both IADC and ISO standards compliance and actual orbital decay estimation compared to empirical Space Surveillance Network observations.

INTRODUCTION

Orbit lifetime prediction is an important component of satellite mission design and post-launch space operations. Numerous orbit propagation tools and atmosphere models are available for orbit lifetime estimation within the CubeSat community, such as STK, the NASA Debris Assessment Software (DAS), detailed numerical integration, and the newly-released CelesTrak orbit lifetime database in support of the published ISO Standard 27852¹, “Space Systems — Estimation of Orbit Lifetime.” In this study, we will examine important aspects of orbit lifetime estimation using a subset of these tools and consider implications for both future CubeSat hardware design, development of concepts of operation and orbital decay modeling.

The long term vitality and viability of the CubeSat community may well depend upon its ability to actively address both real issues and common misconceptions by government and industry associated with the orbital debris threat posed by CubeSats. These issues should be addressed by having the CubeSat community take leadership roles in orbital debris assessment, ensuring that all current and future standards, guidelines and directives are met, and invoking effective mitigation strategies. One such mitigation strategy is to limit post-mission orbit lifetime to prevent debris population growth; this requires the daunting task of orbit lifetime assessment using sophisticated modeling techniques and addressing environmental uncertainty issues.

Many in the CubeSat community have proposed technical solutions to decrease on-orbit lifetime

including tethers, inflatable structures, thin film structures, and propulsion. Since many of these approaches have successfully made it to orbit as part of a CubeSat mission, we can start to evaluate the performance of these approaches. Furthermore, the implementation of other spacecraft subsystems such as antennas, deployable solar panels, structural mass, and attitude control will undoubtedly play a significant role in orbital lifetime – despite the fact that orbital mitigation is rarely considered while engineering these subsystems. These orbital lifetime findings can be incorporated into small satellite community knowledge base for future spacecraft programs to consider.

CUBESAT HISTORICAL MANIFEST

We begin by assembling a compendium of all CubeSats successfully launched to date, shown in Table 1. The CubeSats have been sorted by Space Surveillance Catalog (SSC) number, which also sort it by launch or deployment date. The CubeSat “Form Factor” (e.g., 1U, 2U, 3U) is shown in the fourth column. Adopted mass represents a combination of nominal values with exact/measured values. The average Cross-Sectional Area (CSA) is also provided.

The two shaded lines (SSC 37224 and 37361) did not have TLEs publicly available and were not analyzed for orbit lifetime purposes.

This compendium of CubeSat data was assembled through extensive research into the CubeSat launch manifest and dialog with CubeSat operators from many countries.

Table 1: Compendium of CubeSat Launches to Date

| CS # | SCC # | Name | FF(U) | Launch Vehicle | Deploy Date | Decay Date | Actual Lifetime (days) | Adopted_Mass(g) | g/U | Max CSA (cm^2) | Min CSA (cm^2) | Avg CSA (cm^2) |
|------|-------|----------------|-------|----------------|-------------|------------|------------------------|-----------------|--------|----------------|----------------|----------------|
| 1 | 27842 | DTU-1 | 1 | Rokot | 6/30/2003 | | | 1000 | 1000.0 | 100 | 100 | 150 |
| 2 | 27844 | Cute 1 | 1 | Rokot | 6/30/2003 | | | 1000 | 1000.0 | 100 | 100 | 150 |
| 3 | 27845 | QuakeSat | 3 | Rokot | 6/30/2003 | | | 4402 | 1467.3 | 300 | 100 | 350 |
| 4 | 27846 | AAUSAT-1 | 1 | Rokot | 6/30/2003 | | | 1000 | 1000.0 | 100 | 100 | 150 |
| 5 | 27847 | CanX-1 | 1 | Rokot | 6/30/2003 | | | 1000 | 1000.0 | 100 | 100 | 150 |
| 6 | 27848 | XI-IV | 1 | Rokot | 6/30/2003 | | | 995 | 995.0 | 100 | 100 | 150 |
| 7 | 28892 | UWE-1 | 1 | Kosmos-3M | 10/27/2005 | | | 1000 | 1000.0 | 100 | 100 | 150 |
| 8 | 28895 | XI-V | 1 | Kosmos-3M | 10/27/2005 | | | 1030 | 1030.0 | 100 | 100 | 150 |
| 9 | 28897 | Ncube-2 | 1 | Kosmos-3M | 10/27/2005 | | | 1000 | 1000.0 | 100 | 100 | 150 |
| 10 | 28941 | Cute 1.7+APD | 2 | MV-8 | 2/21/2006 | 10/25/09 | 1342 | 3600 | 1800.0 | 200 | 100 | 250 |
| 11 | 29655 | GeneSat | 3 | Minotaur I | 12/16/2006 | 08/04/10 | 1327 | 5000 | 1666.7 | 300 | 100 | 350 |
| 12 | 31122 | CSTB1 | 1 | Dnepr | 4/17/2007 | | | 900 | 900.0 | 100 | 100 | 150 |
| 13 | 31126 | MAST | 3 | Dnepr | 4/17/2007 | | | 3210 | 1070.0 | 300 | 100 | 350 |
| 14 | 31128 | Libertad-1 | 1 | Dnepr | 4/17/2007 | | | 995 | 995.0 | 100 | 100 | 150 |
| 15 | 31129 | CP3 | 1 | Dnepr | 4/17/2007 | | | 836 | 836.0 | 100 | 100 | 150 |
| 16 | 31130 | CAPE-1 | 1 | Dnepr | 4/17/2007 | | | 851 | 851.0 | 100 | 100 | 150 |
| 17 | 31132 | CP4 | 1 | Dnepr | 4/17/2007 | | | 1019 | 1019.0 | 100 | 100 | 150 |
| 18 | 31133 | AeroCube-2 | 1 | Dnepr | 4/17/2007 | | | 959 | 959.0 | 100 | 100 | 150 |
| 19 | 32787 | Compass-1 | 1 | PSLV-C9 | 4/28/2008 | | | 850 | 850.0 | 100 | 100 | 150 |
| 20 | 32788 | AAUSAT-2 | 1 | PSLV-C9 | 4/28/2008 | | | 750 | 750.0 | 100 | 100 | 150 |
| 21 | 32789 | Delfi-C3 | 3 | PSLV-C9 | 4/28/2008 | | | 2239 | 746.3 | 300 | 100 | 350 |
| 22 | 32790 | CanX-2 | 3 | PSLV-C9 | 4/28/2008 | | | 3476 | 1158.7 | 300 | 100 | 350 |
| 23 | 32791 | SEEDS-2 | 1 | PSLV-C9 | 4/28/2008 | | | 1021.5 | 1021.5 | 100 | 100 | 150 |
| 24 | 35002 | PharmaSat | 3 | Minotaur I | 5/19/2009 | | | 4500 | 1500.0 | 300 | 100 | 350 |
| 25 | 35003 | CP6 | 1 | Minotaur I | 5/19/2009 | | | 990 | 990.0 | 100 | 100 | 150 |
| 26 | 35004 | HawkSat-1 | 1 | Minotaur I | 5/19/2009 | | | 880 | 880.0 | 100 | 100 | 150 |
| 27 | 35005 | AeroCube-3 | 1 | Minotaur I | 5/19/2009 | 01/06/11 | 597 | 1100 | 1100.0 | 100 | 100 | 150 |
| 28 | 35932 | SwissCube | 1 | PSLV-C9 | 9/23/2009 | | | 820 | 820.0 | 100 | 100 | 150 |
| 29 | 35933 | BeeSat | 1 | PSLV-C9 | 9/23/2009 | | | 936 | 936.0 | 100 | 100 | 150 |
| 30 | 35934 | UWE-2 | 1 | PSLV-C9 | 9/23/2009 | | | 1058 | 1058.0 | 100 | 100 | 150 |
| 31 | 35935 | ITU-pSat | 1 | PSLV-C9 | 9/23/2009 | | | 960 | 960.0 | 100 | 100 | 150 |
| 32 | 36573 | Hayato (K-Sat) | 1 | H-IIA | 5/20/2010 | 06/28/10 | 39 | 1400 | 1400.0 | 100 | 100 | 150 |
| 33 | 36574 | Waseda-Sat2 | 1 | H-IIA | 5/20/2010 | 07/12/10 | 53 | 1150 | 1150.0 | 100 | 100 | 150 |
| 34 | 36575 | Negai | 1 | H-IIA | 5/20/2010 | 06/26/10 | 37 | 986.4 | 986.4 | 100 | 100 | 150 |
| 35 | 36796 | StudSat | 1 | PLSV-CA | 7/12/2010 | | | 850 | 850.0 | 100 | 100 | 150 |
| 36 | 36799 | Tisat-1 | 1 | PLSV-CA | 7/12/2010 | | | 995 | 995.0 | 100 | 100 | 150 |
| 37 | 37224 | O/OREOS | 3 | Minotaur IV | 11/20/2010 | | | 5500 | 1833.3 | 300 | 100 | 350 |
| 38 | 37245 | QbX2 | 3 | Falcon 9 | 12/8/2010 | 01/16/11 | 39 | 4516 | 1505.3 | 300 | 100 | 350 |
| 39 | 37246 | SMDC-ONE | 3 | Falcon 9 | 12/8/2010 | 01/12/11 | 35 | 4050 | 1350.0 | 300 | 100 | 350 |
| 40 | 37247 | PERSEUS 003 | 1.5 | Falcon 9 | 12/8/2010 | 12/31/10 | 23 | 1500 | 1000.0 | 150 | 100 | 200 |
| 41 | 37248 | PERSEUS 001 | 1.5 | Falcon 9 | 12/8/2010 | 12/31/10 | 23 | 1500 | 1000.0 | 150 | 100 | 200 |
| 42 | 37249 | QbX1 | 3 | Falcon 9 | 12/8/2010 | 01/06/11 | 29 | 4529 | 1509.7 | 300 | 100 | 350 |
| 43 | 37250 | PERSEUS 002 | 1.5 | Falcon 9 | 12/8/2010 | 12/30/10 | 22 | 1500 | 1000.0 | 150 | 100 | 200 |
| 44 | 37251 | PERSEUS 000 | 1.5 | Falcon 9 | 12/8/2010 | 12/30/10 | 22 | 1500 | 1000.0 | 150 | 100 | 200 |
| 45 | 37252 | MAYFLOWER | 3 | Falcon 9 | 12/8/2010 | 12/22/10 | 14 | 4750 | 1583.3 | 300 | 100 | 350 |
| 46 | 37361 | NanoSail-D2 | 3 | Minotaur IV | 11/20/2010 | | | 4000 | 1333.3 | 300 | 100 | 350 |
| 47 | 90021 | RAX (37223) | 3 | Minotaur IV | 11/20/2010 | | | 2833 | 944.3 | 300 | 100 | 350 |

The number of CubeSats launched is shown in Figure 1. As the figure shows, the number of on-orbit CubeSats declined last year for the first time since the beginning of the CubeSat program.

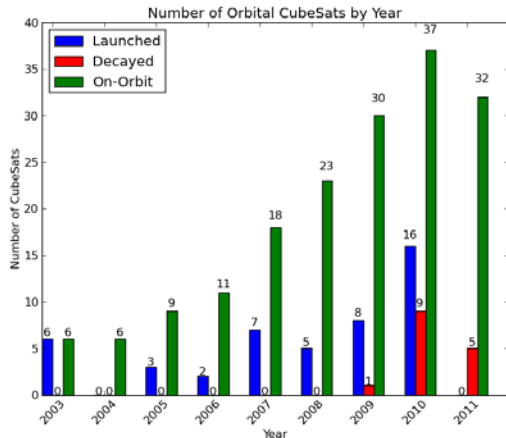


Figure 1: Orbital CubeSats by Year

The relationship between CubeSat mass and CubeSat form factor is examined in Figure 2. The 3U CubeSats vary the most in mass.

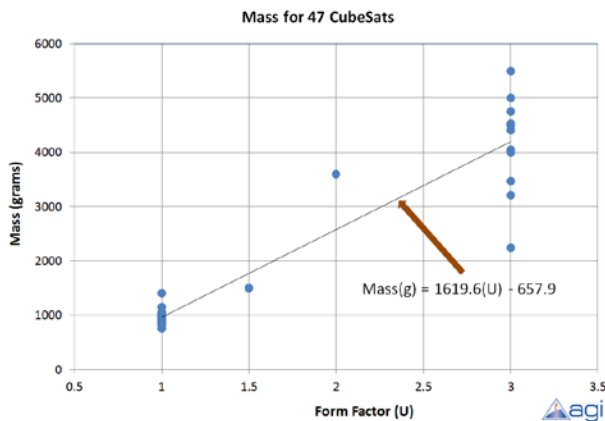


Figure 2: CubeSat Mass-to-Form Factor Relationship

RESIDENT SPACE OBJECT POPULATION

For CubeSat designers, builders and operators, it is of interest to examine the existing population of satellites and space debris in the Low Earth Orbit (LEO) regime.

We begin by examining the evolution the space population in Figure 3. The debris-generating Cosmos/Iridium collision and Chinese Fengyun satellite intercept events are easily observed in the figure.

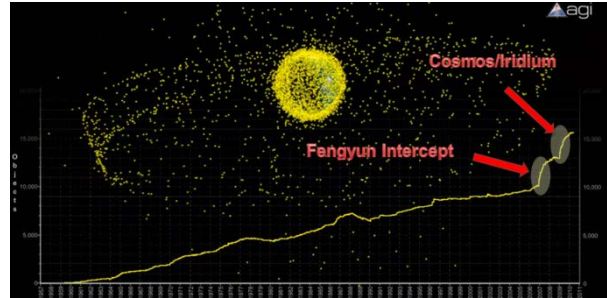


Figure 3: Evolution of the Resident Space Population from 1957 to Present

The distribution of the LEO space population is examined in Figure 4². The various spikes in the population due to large satellite constellations (e.g., Iridium, Orbcomm) and debris populations is seen in the figure.

RSO Perigee Altitude Distribution versus Apogee Altitude (LEO)
(8 km bins, 1957-2011, LEO Only, Inc: 0° - 110°, All RCS values)

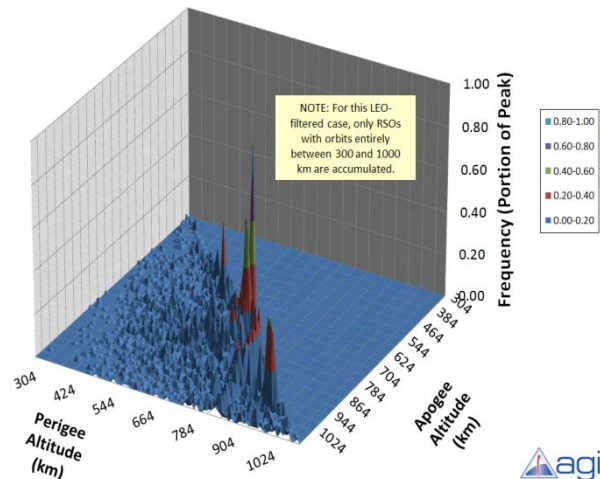


Figure 4: Three-Dimensional View of LEO Space Population Distribution

In Figure 5, the LEO distribution is viewed from above and combined with a 25-year median orbit lifetime curve based upon a sample “average” ballistic coefficient derived from Ref. 3. In this depiction, the horizontal and vertical banding typically seen in post-collision Gabbard plots are easily identified for both the Cosmos/Iridium collision and the Fengyun intercept event. Unfortunately, one can easily see that this debris is now essentially a permanent fixture in our orbital debris environment.

RSO Perigee Altitude Distribution versus Apogee Altitude (LEO)

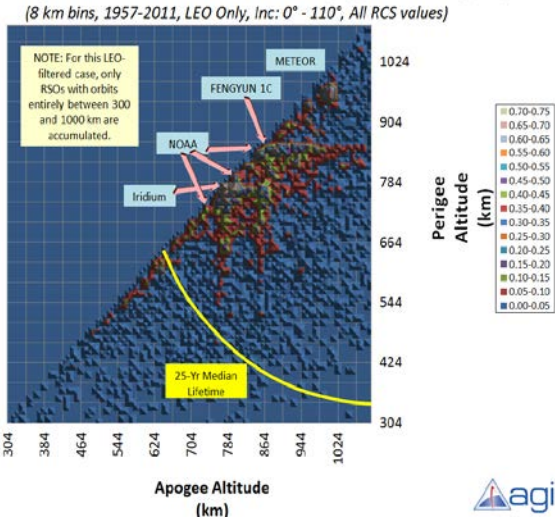


Figure 5: LEO Distribution With 25-Year Median Orbit Lifetime for Sample Ballistic Coefficient

It is also of interest to examine a plot of space object spatial density. As discussed in Ref. 2, the space population is shown to be most dense in the LEO (i.e. less than 2000 km altitude) and Geosynchronous Earth Orbit (GEO, at 35,000 km altitude) regions, as shown in Figure 6.

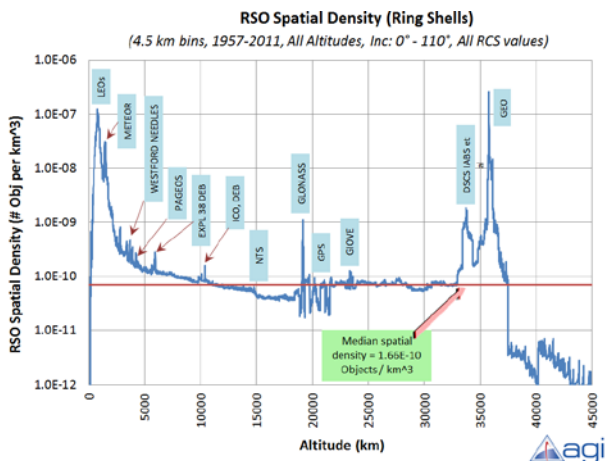


Figure 6: Space Object Spatial Density

One can use spatial density data to estimate collision probability. Although many assumptions must be made to map spatial density into collision probability, the result is illustrative nevertheless as shown in Figure 7. Interestingly, close examination of the figure shows that although spatial density is higher at GEO than at LEO, the collision probability is higher at LEO because LEO satellites orbit fifteen times in a day while GEO orbits the Earth only once per day.

Collision Probability Against Currently-Tracked RSOs

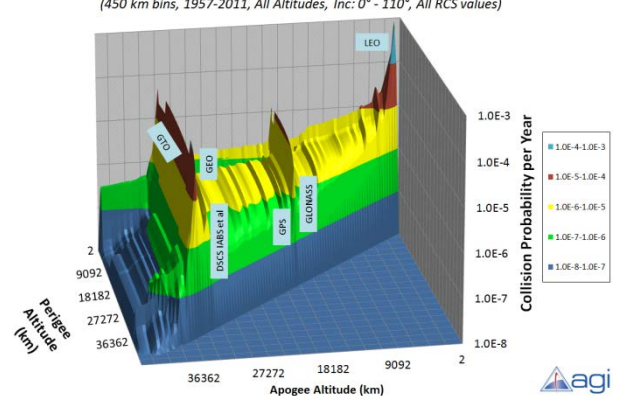


Figure 7: Space Object Collision Probability

ORBIT LIFETIME COMPUTATIONS FOR CUBESATS

Why the CubeSat Community should be Concerned with Orbital Debris...

The CubeSat community has a vested interest in ensuring the safe and enduring use of and access to space. We must address the broader space communities’ view that CubeSats pose both real and perceived orbital debris threats to other government and industry space operations.

The CubeSat community must avoid any concepts or perceptions that it advocates carelessly-deployed “swarms of picosatellites” or other phased-array CubeSat constellations if it does not first carefully plan those missions to avoid the creation of lasting space debris. A former colleague, Dr. E.Y. Robinson, coauthored an article⁴ which advocated the use of such a “swarm” of thousands of satellites orbiting at 700 km altitude. The following editorial (Figure 8) was posted in reply, by none other than Arthur C. Clarke.

As another example, one of this paper’s authors was lead Tracking analyst for The Aerospace Corporation’s picosatellite tethered pair (each the size of a deck of cards), as deployed in 1999 from Stanford’s OPAL spacecraft. That same author also co-developed the nation’s launch collision window screening tool Collision Vision, still in use today for all US DoD and National launches. At the time a believer that space is “big”, imagine the surprise when the US had to hold a launch because of a would-be conjunction between the picosatellite pair and the Titan/Centaur-launched, billion-dollar mission. A key realization is that while the likelihood of collision would have been small, the mere existence of a chance of collision is sufficient to make our operations in space more difficult.

I was appalled by the article **Big benefits from tiny technologies** in the October 1996 issue (p. 38). Have the writers stopped to think about the implications of “thousands of satellite constellations orbiting, for example, at 700 km altitude”? For a long time I have been worried about such projects as Iridium, which only proposed 77 (though now I see it's 161!). And as for Teledesic...words fail me.

I have already suggested that future space travelers may have to pass through orbiting mine fields. Now what's suggested is even worse—orbiting dust storms!

Although I am understandably biased in favor of geostationary satellites, I feel that the benefits of LEO satellites are exaggerated. They have no power advantage over GEO satellites, if spot beams are employed, and their one undoubted superiority is in the reduced time delay. If space travel develops as we all hope it will, they may have to be banned in the next century, as a hazard to navigation.

For the ultimate solution, see “3001: The Final Odyssey!”

Arthur C. Clarke
Sri Lanka

Figure 8: Arthur C. Clarke Editorial

Such perceptions can be addressed by:

- Ensuring that CubeSats are packed with as much utility and capabilities as we can endow them with (use space wisely!);
- Taking leadership roles in orbital debris assessment;
- Ensuring all current and future orbital debris mitigation standards, guidelines and directives are met;
- Avoid mission orbits that prevent near-term natural decay;

- Limit post-mission orbit lifetime to prevent debris population growth using sophisticated modeling incorporating environmental uncertainty;

Orbital Debris and Lifetime: What’s the Connection?

The orbital debris population has a direct dependence upon the orbit lifetime of objects positioned in various orbit regimes. LEO satellite orbits are affected primarily by atmospheric drag, with decreasing impact above 650 km.

This was recognized by the Inter-Agency Space Debris Coordination Committee (IADC), which recommends⁴⁵ that spacecraft exit LEO-crossing regime (0 - 2000km) within 25 years of end-of-life (EOL). This may be accomplished in a number of ways, including:

- De-orbit or maneuver to suitably reduce orbit lifetime;
- Dispose in orbit where drag/perturbations will limit lifetime.

Unfortunately, these IADC ‘guidelines’ are recommended best practice, with no regulatory requirement.

In order to provide stronger standard operations directives for orbital debris mitigation, the International Standards Organization (ISO) TC20/SC14/Working Group 3 joined forces with the newly-formed Orbital Debris Coordination Working Group (ODCWG) to help coordinate conversion of IADC guidelines into ISO WG standards. One of the ISO standards developed out of this joint effort is ISO standard 27852^{4,5} covering the computation of orbit lifetime.

CubeSat Orbit Lifetime Uses

Pertaining to orbit lifetime estimation, CubeSats present several unique aspects. The aspect of most interest is that they are in a standardized form factor and mass is well known due to a typical lack of propellant or other mass consumables.

There are generally three reasons for the space community to estimate orbit lifetime:

- Demonstrate compliance with Standards or Best Practices;
- Predict a future (actual) orbit demise;
- Post-decay forensic analysis and ballistics characterization;

Selection of the above reason for the computation generally dictates the type of space weather profile(s) to be used for the analysis. For example, one could use “typical” atmosphere profiles when evaluating ISO

standards compliance and design. If the analyst’s goal is to guarantee compliance, worst-case space weather indices could be adopted. Alternately, forensic analysis of real orbital decay profiles requires the use of best-available, actual space weather parameters.

Orbit Lifetime Analysis Components

The key components required to estimate orbit lifetime are shown in Figure 9. A number of orbit lifetime tools exist with varying degrees of accuracy and realism; models we’re using include the Earth QuickProp (QProp) propagator, supporting the published ISO Standard 27852, “Space systems — Estimation of orbit lifetime,” STK’s orbit lifetime estimator, detailed numerical integration from STK and other orbit propagation packages, the NASA Debris Assessment Software (DAS), and others. Note that a future deployment of a digital orbit lifetime database will soon be available on www.CelesTrak.com.

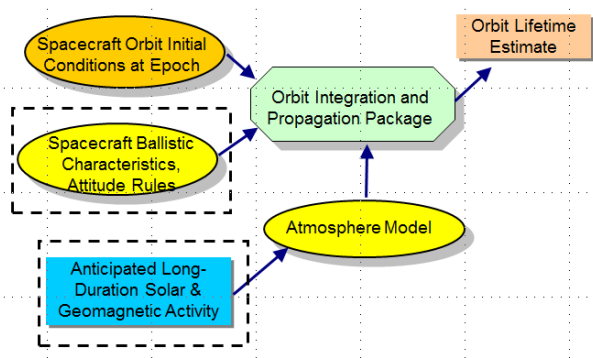


Figure 9: Orbit Lifetime Analysis Components

The two components in Figure 9 surrounded by the dotted rectangle represent areas that we will focus on due to their complexity to the analyst.

Orbit Lifetime Approaches

Three primary methods exist to estimate orbit lifetime.

In Method 1, direct numerical integration of a full complement of detailed perturbing forces can be accomplished in Cartesian space. This approach is the most detailed and can include force models for the gravity geopotential, third-body effects, Solar Radiation Pressure (SRP), and vehicle-dependent, attitude rules-based ballistic coefficient definitions.

In Method 2, semi-analytic propagation of mean orbit elements influenced by gravity zonals J2 thru J7 may be coupled with orbit-averaged drag, third-body and SRP perturbations.

In Method 3, summary tables, graphs, and/or fit equations produced using Methods 1 and 2 may be used

to roughly estimate orbit lifetime. Method 1 analyses typically require substantially more time to run than Methods 2 & 3.

In cases where high-eccentricity orbits or other orbits exploiting Earth resonance effects are present, Method 1 computations are recommended. In all other cases, the analyst is usually rewarded by the selection of a suitable Method 2 approach. In Figure 10, output from Methods 1 and 2 are overlaid using identical atmosphere models and space weather coefficients. As noted in the figure, Method 2 was 780 times faster than Method 1 for virtually the identical result.

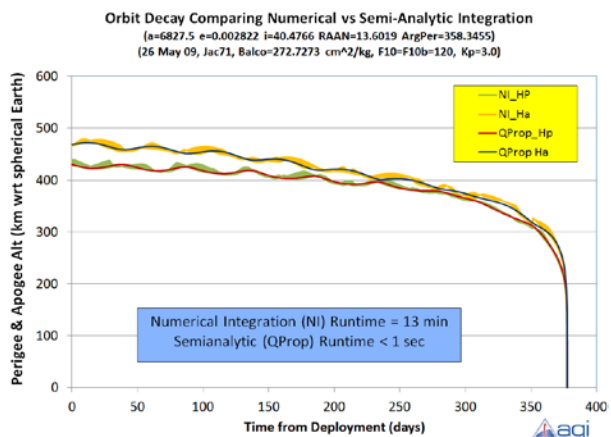


Figure 10: Orbit Lifetime Method 1 & 2 Comparison

Spacecraft Ballistic Coefficient Modeling

The first step in estimating CubeSat orbit lifetime is to estimate the ballistic coefficient β , where:

$$\beta = \left[\frac{C_D \cdot \text{Cross-Sectional Area (cm}^2\text{)}}{\text{mass (kg)}} \right] \quad (1)$$

Accurate estimation of the space object’s ballistic coefficient is a key element in the orbit lifetime analysis process. Frequently, the analyst will select an average ballistic coefficient for the duration of the prediction, but this is not always the case. We will examine each component (the drag coefficient C_D , and cross-sectional area). Spacecraft mass shall be varied according to best-available knowledge, but may typically be assumed to be constant from End-of-Life until orbit decay.

Estimating drag coefficient

A reasonable value of the dimensionless drag coefficient, C_D , is 2.2 for a typical spacecraft. However,

the drag coefficient, C_D , depends on the shape of the satellite and the way air molecules collide with it. The analyst shall consider C_D variations based on satellite shape. However, for long-duration orbit lifetime estimations, C_D variation as a function of orbit altitude may safely be ignored since the orbit lifetime percent error will be quite small due to averaging effects about the adopted 2.2 value.

Estimating cross-sectional area with tumbling and stabilization modes

If the attitude of the spacecraft can't be anticipated (as is typically the case), the user should compute a mean cross-sectional area assuming that the attitude of the spacecraft may vary uniformly (relatively to the velocity direction) The mean cross-sectional area is obtained by integrating the cross-sectional area across a uniform distribution of attitude of the spacecraft (as if an observer would observe a spacecraft from any direction and compute the resulting mean observed cross-section).

In the absence of a more detailed model, a composite flat-plate model may be utilized. For example, for a plane sheet of which S is the area, it can be demonstrated that the "mean surface area" is $S/2$ when averaged over all possible viewing angles; by extension, for a parallelepiped-shaped spacecraft, S_1, S_2, S_3 being the three surfaces (their opposite sides are to be neglected because when a side is visible):

$$CSA = \frac{1}{2} [S_1 + S_2 + S_3 (+ S_4 + \dots)] \quad (2)$$

If a solar array of surface S_4 is added, the mean surface area is then $(S_1+S_2+S_3+S_4)/2$ (neglecting any possible masking between the solar array and the spacecraft). This flat plate model has been shown to be accurate to within 20% for tracked objects. Since masking effects represent a systematic bias that has the effect of reducing drag (thereby increasing orbit lifetime), an appropriately conservative cross-sectional area masking reduction factor shall be introduced to maintain accuracy.

To eliminate the need for such conservatism, this plate model approach can be extensively refined by integrating the cross-sectional area of the spacecraft across all anticipated tumbling attitudes (e.g. using a Computer-Aided Design or CAD program), and then dividing the result by the difference between the limits of integration. The analyst is then left with a properly weighted average cross-sectional area.

For satellites with a large length to diameter ratio, the analyst shall consider whether gravity-gradient stabilization will occur and adjust the cross-sectional

area based upon the anticipated stabilized geometry. Similarly, for satellites which have a large aero-torque moment (*i.e.*, the center-of-gravity and center-of-pressure are suitably far apart and the aerodynamic force is suitably large), the analyst shall consider whether the satellite would experience drag-induced passive attitude stabilization and adjust the cross-sectional area accordingly.

Atmosphere Models

There are a wide variety of atmosphere models available for orbit lifetime estimation purposes. As we will demonstrate, it is important to employ a dynamic atmosphere model in such analyses. Use of the more recent atmosphere models are encouraged because they have substantially more atmospheric drag data incorporated as the foundation of their underlying assumptions. The reader is encouraged to seek atmosphere model guidance from existing and upcoming ISO Standards⁶ and CIRA Working Group (e.g. CIRA-2008) recommendations. Models worthy of consideration include, but are not limited to, the NRLMSISE-00⁷, JB2006⁸, JB2008⁹, GRAM-07¹⁰, DTM-2000¹¹ and GOST¹² models. For the remainder of this paper, we will select the non-dynamic 1976 Standard Atmosphere, Jacchia 1971, Jacchia-Bowman 2006 and MSISE2000 atmosphere models.

Space Weather Modeling

In addition to atmosphere modeling uncertainties for known space weather conditions, a lack of knowledge and unpredictability in space weather conditions leads to large uncertainties in orbit lifetime estimation. An example of this unpredictable nature is shown in Figure 11. The figure shows that while a averaged 3905-day solar cycle exists with an averaged solar minimum occurring at approximately 25 May 2008 (derived by the author based upon data extracted from Ref. 13), the level of solar activity within each cycle is highly variable.

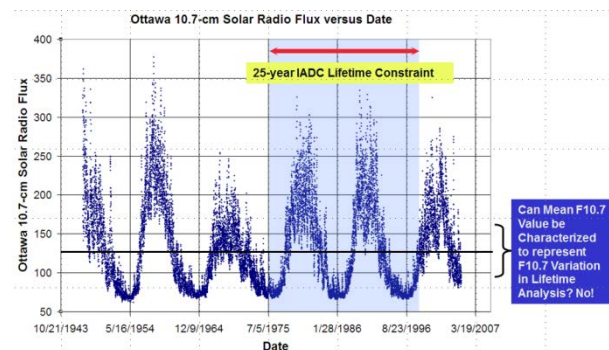


Figure 11: Solar Radio Flux at 10.7 cm

And although the minimum and maximum boundaries for the solar cycle indices could be readily hand-drawn (as shown in Figure 12), a more important question is what is the distribution of indices in the vertical direction at any point in the cycle?

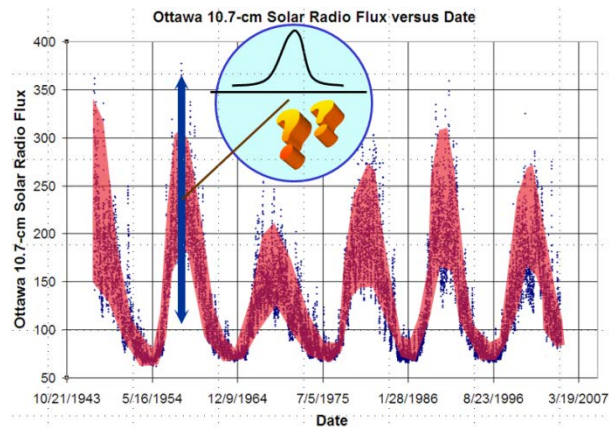


Figure 12: Hand-Drawn Solar Radio Flux Regions

Post-processing of the F10.7 data from 1947 to 2006 inclusive shows (Figure 13) that the distribution favors low solar activity; this means that although high solar activity definitely occurs, it is not as frequent as compared to typical solar activity.

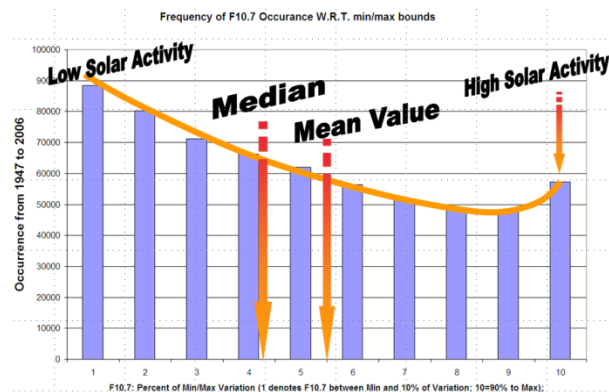


Figure 13: Solar Radio Flux Vertical Distributions

An important conclusion from Figure 13 is that using long-range minimum, percentile and/or maximum space weather forecasts as shown in , such as may be obtained from Ref. 14 may be misleading because the actual “median” value is not well-represented by the “average” value shown in Figure 14.

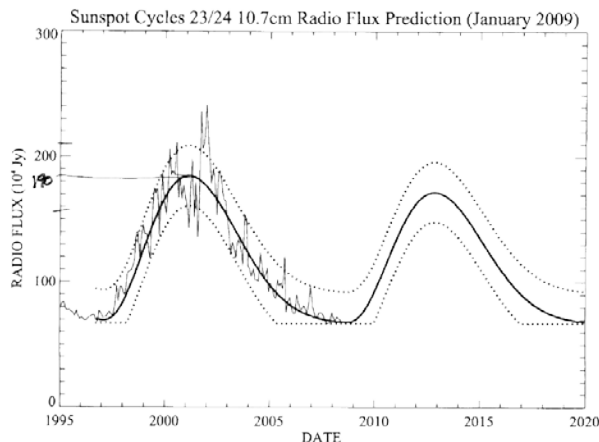


Figure 14: Radio Flux Long-Range Predictions

The recommended Best Practice for accommodating such space weather uncertainty is to use the past 64 years of space weather data already collected and perform random draws of the data (keeping solar and geomagnetic indices paired together for a given day of interest), representing the “day within a modulo-ed cycle” as shown in Figure 15 and Figure 16.

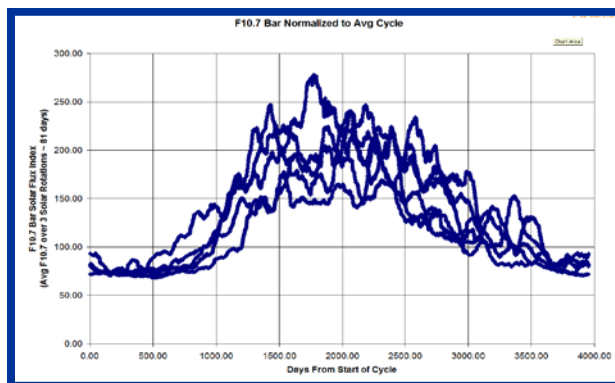


Figure 15: F10.7 Bar Radio Flux Normalized to Average Solar Cycle

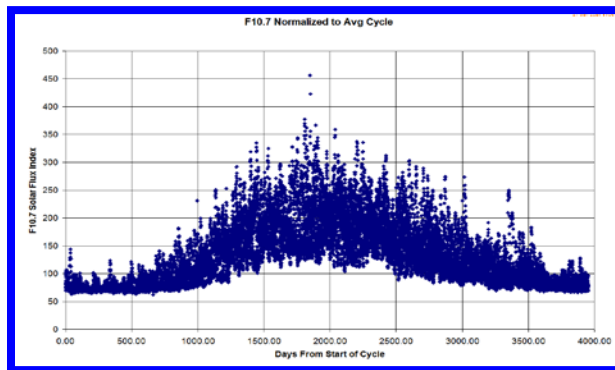


Figure 16: F10.7 Radio Flux Normalized to Average Solar Cycle

Conducting such random draws of the space weather coefficients for millions of orbit lifetime analysis runs yields Figure 17.

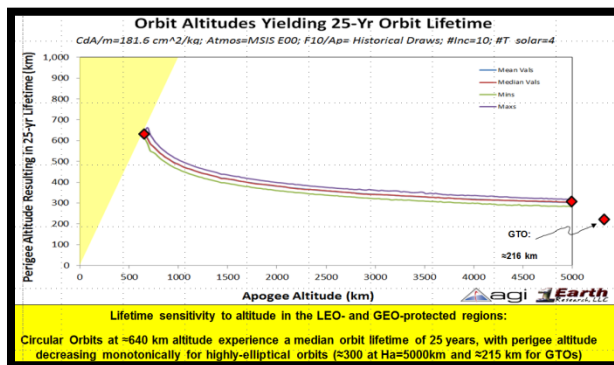


Figure 17: Orbit Altitudes Yielding 25-Year Orbit Lifetime for Sample Ballistic Coefficient

CubeSat Orbit Lifetime Analysis Approach

There are 47 CubeSats in Table 1. Of those 47, we will discard two due to a lack of available TLEs for them.

The masses of almost all remaining 45 CubeSats are known. And, due to the standardized CubeSat form factor, we can use equation (2) to compute average cross-sectional area (and have done so, as provided in Table 1).

Our analysis approach consists of selecting one or more semi-analytic orbit propagators, selecting an atmosphere model, assume that the CubeSats are randomly tumbling (i.e., Eqn. 2 is valid) and using existing public CelesTrak data (www.CelesTrak.com) to evaluate actual orbital decay. For this initial study, the IEarth Quick-Prop propagator was selected. A static atmosphere model (Standard Atmosphere 1976) was chosen for purposes of illustration to show why only selecting dynamic atmosphere models is important. Other selected atmosphere models were Jacchia 1971, MSISE2000, and Jacchia-Bowman 2006. For the JB2006 model, note that standard F10, F10bar and Ap values were input per guidance from the developer. Application of the more accurate X and S space weather coefficients which can feed JB2006 will be undertaken in a follow-on study.

Another approach we could have adopted is depicted in Figure 18. The figure shows the orbit lifetime a CubeSat would experience as a function of the drag coefficient modeled, yet in this sample case we know the orbit lifetime to be 1.61 years. By determining how orbit lifetime varies parametrically based upon C_D , the intersection of that parametric line with the actual orbit lifetime indicates the estimated drag coefficient C_D .

Instead, we opted to minimize the semi-major axis residuals throughout the CubeSat decay to determine the drag coefficient which best fits the observed data. Prior to optimal drag coefficient optimization, outlier element sets are discarded using the technique presented in Ref. XXX. Upon completion, the drag coefficient for each CubeSat are optimally estimated for each drag model in order to minimize semi-major axis decay residuals.

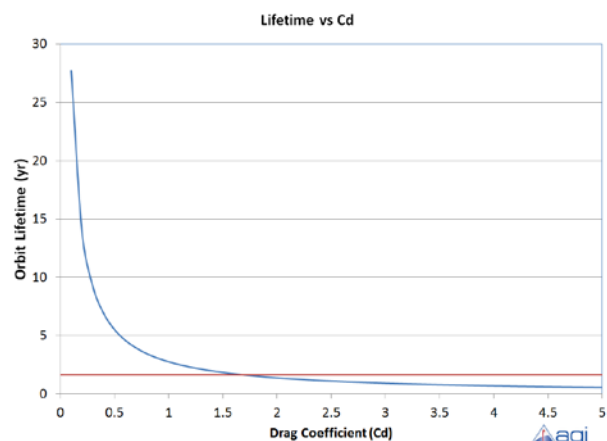


Figure 18: F10.7 Parametric Lifetime Study vs C_D

CubeSat Orbit Lifetime Analysis Results

If the selected atmosphere model had perfect knowledge and our random attitude tumble assumption was perfectly accurate, then the resultant C_D solutions would be extremely stable. As a result, we can examine the instability of the C_D solution for a number of cases to determine atmospheric model biases and inaccuracies, since values far from a nominal value of perhaps 2.2 are suspect. The results for the selected analysis approach are shown in Figure 19 through Figure 22.

The figures depict the variability in the solved-for C_D solution for each of the four atmosphere models, as a function of case number (Figure 19), residual error (Figure 20), form factor (Figure 21) and perigee altitude (Figure 22).

The poor performance of the static Standard Atmosphere 1976 is readily apparent, since it has a wide and unfocused distribution. The performance of the other three atmosphere models is much better, with all three performing sufficiently for our purposes. A slight bias in the C_D solution can be observed, in that the C_D for JB2006 appears to be about 20% higher than that of MSISE2000 and Jacchia 1971 models.

It's worth noting that the majority of drag coefficient estimation cases with high residuals were later determined to have external appendages (deployable

antennas, drag enhancement devices, or other drag-modifying characteristics. As QProp was artificially capped at a maximum drag coefficient of 5, this had the effect of preventing ballistic coefficient from being determined as optimally as it could have been.

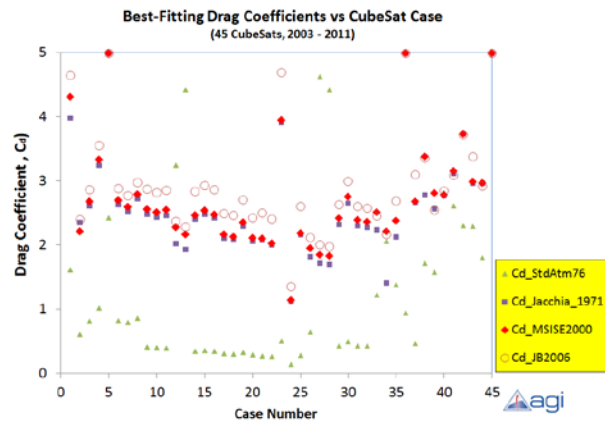


Figure 19: Drag Coefficient vs. Case Number

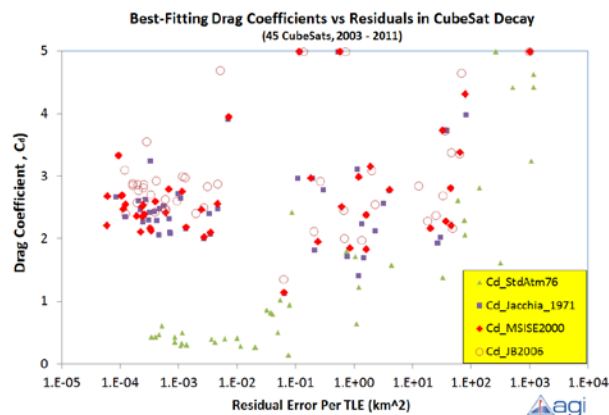


Figure 20: Drag Coefficient vs. Residuals

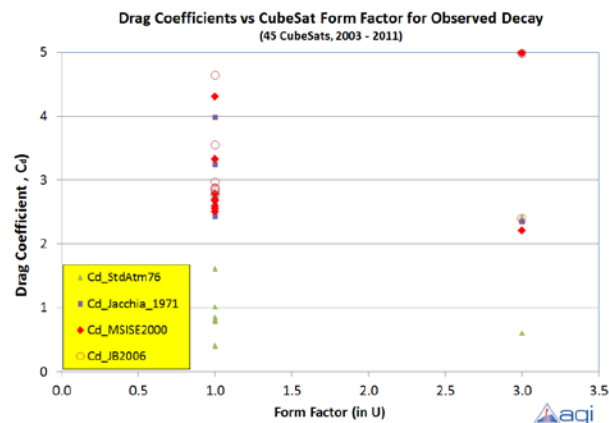


Figure 21: Drag Coefficient vs. Form Factor

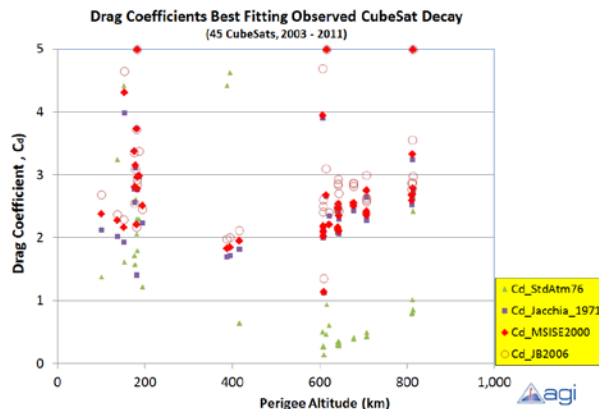


Figure 22: Drag Coefficient vs. Perigee Altitude

Comparison of Orbit Lifetime Estimation Models

Now that drag coefficients have effectively been optimally determined for each decay case, the initial orbit and the solved-for drag coefficients consistent with a selected atmosphere model can be entered into orbit lifetime estimation models. For this study, the NASA Debris Assessment Software (DAS), AGI's STK software and IEarth's QProp lifetime estimation tools were adopted. Where the atmosphere model was selectable, the MSIS 2000 model was used; solved-for drag coefficients (using the corresponding MSIS 2000 atmosphere with QProp) were input into the models. Note that the DAS package doesn't permit drag coefficient numbers to be input, which leads to an inevitable loss of accuracy with respect to the other models.

The results of the comparison are shown in Figure 23. The lifetime predictions have been normalized to the orbit lifetime actually observed, such that a ratio of one (depicted by the red line) represents a perfect lifetime prediction. The orbital decays to the left of the orange shaded region are multi-year decays (3.7, 3.6, and 1.7 years, respectively), whereas those inside of the orange region are for actual decays spanning roughly one month or less.

Note that this approach slightly favors the QProp predictions, since the drag coefficient was optimized using QProp. Note also that the predictions match quite well for the long-duration predictions.

Short-term decays were predictably poorer in performance with respect to the actual decay. Of the three lifetime prediction models, QProp and STK matched the actual decay. But this may be attributed in part to QProp's and STK's ability to combine the MSIS atmosphere model with self-consistent drag coefficients for each CubeSat, coupled with DAS's inability to ingest any vehicle-specific drag coefficient data.

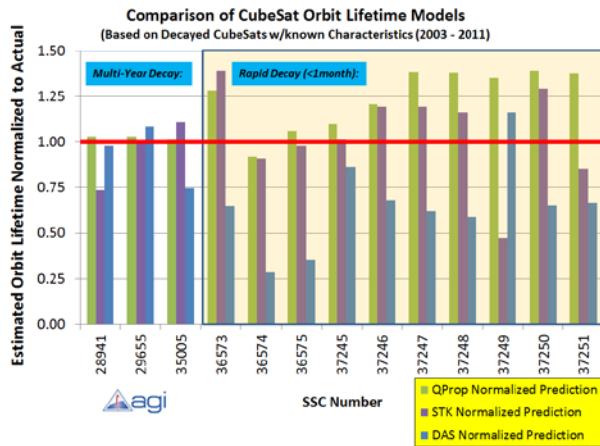


Figure 23: Lifetime Model Comparison

Implications of the “CubeSat Launch Quandary”...

If you’ve been a part of the CubeSat community, you realize that the most difficult aspect to being able to operate your CubeSat in space is trying to arrange a launch for your vehicle. There is an enormous economy of scale regarding launch weight: Launch and insertion of a tiny mass to orbit is very expensive (especially on a per-kilogram basis!), but putting up two or more of the tiny mass objects costs can be achieved at little or no additional cost. This has led to the “primary/secondary payload” concept, which has greatly increased access to space for the CubeSat community. Unfortunately, the primary payload almost always gets to choose the orbit that the launcher delivers their satellite to, so unless the launcher can deploy the CubeSats in a separate orbit, the CubeSats will obtain roughly the same orbit as the primary.

This presents a problem from a debris mitigation standpoint, since CubeSats typically do not have a deorbit module or powered tether to facilitate meeting the ISO standard 25-year post-mission orbit lifetime rule. The CubeSat community should encourage such missions as the Von Karman Institute’s QB50 mission, which has purchased a single launcher whose mission profile is tailored solely to the CubeSat community and whose typical mission orbit lifetimes are on the order of several months. This will yield a sustainable use of LEO space.

So how has the CubeSat community done with respect to current IADC guidance, ISO standards and orbital debris mitigation? To date, the community has not done well in addressing these important issues. Figure 24 is a reposting of Figure 5 but with 45 icons for each CubeSat deployed to date (minus the two for which TLEs were unavailable). As the red icons show, only thirty-eight percent of all CubeSats launched to-date

will provide a sufficiently short orbital lifetime to help protect our fragile space environment.

RSO Perigee Altitude Distribution versus Apogee Altitude (LEO)
(8 km bins, 1957-2011, LEO Only, Inc: 0° - 110°, All RCS values)

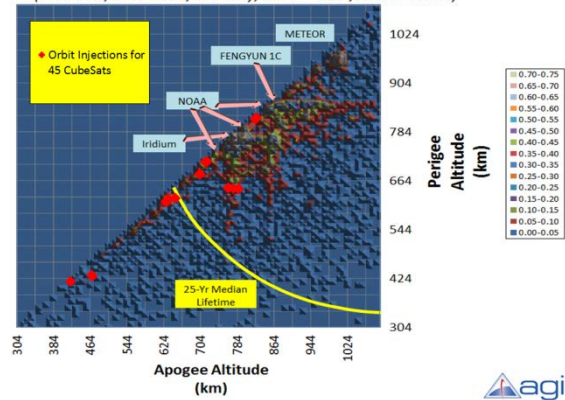


Figure 24: CubeSat Apogee/Perigee Distribution

Conclusions

In this paper, the importance of orbit lifetime computation and associated debris mitigation issues for the CubeSat community has been discussed. It has also been demonstrated that CubeSats provide a convenient platform by which to explore a variety of orbit lifetime and atmosphere modeling and accuracy issues.

Typical ballistic coefficient variations are roughly consistent with the suggested 20% accuracy guideline for the adopted cross-sectional area equation (2).

Action must be taken to modify current CubeSat-as-a-secondary-payload deployment schemes and practices to avoid needless space debris population growth.

The need for additional work in the CubeSat orbit lifetime topic is indicated by this study, including analysis of additional atmosphere models (JB2008, GOST, GRAM, etc) and more refined cross-sectional area models for CubeSats having deployable appendages..

Acknowledgments

The authors would like to thank the contributions of the many CubeSat builders and operators for contributing information to the CubeSat compendium in Table 1.

References

1. ISO Standard 27852, “Space Systems – Determining Orbit Lifetime, International Organization for Standardization, Geneva, Switzerland, 2009.
2. Oltrogge, D.L. and Kelso, T.S., “Getting to know our space population from the public catalog,”

- 2011 AAS/AIAA Astrodynamics Conference, Girdwood, AK, August 2011.
3. Wiedemann, C., et. al., Cost of Particle Impacts on a Satellite, Institute of Aerospace Systems, Technische Universitat Braunschweig, 20 April 2005.
 4. Robinson, E.Y. and Janson, S., "Big Benefits from Tiny Technologies," Aerospace America, October 1996.
 5. IADC Space Debris Mitigation Guidelines, Inter-Agency Debris Coordination Committee, IAD-02-01, Rev 1, Sep 2007.
 6. Oltrogge, D.L. and Chao, C.C., "Standardized Approaches for Estimating Orbit Lifetime after End-of-Life," AAS/AIAA Astrodynamics Conference, Mackinac Island, MI, August 2007.
 7. Finkleman, D. and Oltrogge, D.L., "Twenty-five Years, More or Less: Interpretation of LEO Debris Mitigation 25-Year Post-Mission Lifetime Guideline," AAS/AIAA Astrodynamics Conference, Toronto, Canada, August 2010.
 8. ISO Draft Standard 14222, "Space systems – Space Environment (natural and artificial) – Earth Upper Atmosphere", International Organization for Standardization, Geneva, Switzerland, 2011.
 9. J.M. Picone, A.E. Hedin, D.P. Drob, and A.C. Aikin, "NRL-MSISE-00 Empirical Model of the Atmosphere: Statistical Comparisons and Scientific Issues," J. Geophys. Res., doi:10.1029/2002JA009430, in press (2003).
 10. Bowman, B. R., Tobiska, W. K., Marcos, F. A., Vallares, C. The JB2006 empirical thermospheric density model, *Journal of Atmospheric and Solar-Terrestrial Physics* 70 (5), 774-793, 2008.
 11. Bowman, B. R., Tobiska, W. K., Marcos, F. A., Huang, C.Y., Lin, C.S. & Burke, W.J., New Empirical Thermospheric Density Model JB2008 Using New Solar and Geomagnetic Indices, AIAA 2008-6438, AIAA/AAS Astrodynamics Specialist Conference, Honolulu, Hawaii, August 2008.
 12. Justus, C.G. and Leslie, F.W., The NASA MSFC Earth Global Reference Atmospheric Model—2007 Version, NASA/TM—2008–21581, November 2008.
 13. Bruinsma, S., Thuillier, G., and Barlier, F., The DTM-2000 empirical thermosphere model with new data assimilation and constraints at lower boundary: accuracy and properties, *Journal of atmospheric and solar-terrestrial physics* ISSN 1364-6826, 2003, vol. 65, no. 9, pp. 1053-1070.
 14. Cefola, P., Volkov, I. I., and Suevalov, V. V., Description of the Russian Upper Atmosphere Density Model GOST-2004, 37th COSPAR Scientific Assembly, Montreal, Canada, July, 2008.
 15. Hathaway, D.H., "The Solar Cycle," NASA Marshall Space Flight Center, Living Rev. Solar Phys., 7, (2010), 1, Published 2 March 2010.
 16. Nassiz, B.J., Berry, K., and Schatten, K, ORBIT DECAY PREDICTION SENSITIVITY TO SOLAR FLUX VARIATIONS, AIAA/AAS Paper 07-264, AAS/AIAA Astrodynamics Specialists Conference, Mackinac Island, MI, August 2007.
 17. Oltrogge, D.L. and Alfano, S.A., "Determination of Orbit Crosstag events and Maneuvers With Orbit Detective," AAS/AIAA Astrodynamics Specialist Conference, Girdwood, AK, August 2011.